Supporting Online Material for

Dystroglycan Function Requires Xylosyl- and Glucuronyltransferase Activities of LARGE

Kei-ichiro Inamori, Takako Yoshida-Moriguchi, Yuji Hara, Mary E. Anderson, Liping Yu, Kevin P. Campbell*

*To whom correspondence should be addressed. E-mail: kevin-campbell@uiowa.edu

Published 6 January 2012, *Science* **335**, 93 (2011)
DOI: 10.1126/science.1214115

This PDF file includes

Materials and Methods

cDNAs

The full-length LARGE expression vector has been described elsewhere (7, 19). Human UXS1 (NM_025076.3, pCMV6 vector, Myc-DDK-tagged) was purchased from Origene.

LARGEdTM constructs and establishment of stable cell lines

LARGEdTM

The construct expressing LARGE without its transmembrane region was generated by amplifying cDNA fragments of human LARGE from pIRES-puro3 LARGE-myc (19) using primer pairs (#7217: 5'-GAACGCGGCCGCTTTCGAAGATGGAAAGCCCG- 3' and #2998: 5'-TTGGCAGGAAGAGTCTTGGT-3' to produce the left fragment; and #3000: 5'-AAGTTTCCTGGATCCCCAAT-3' and #4112: 5'-TTGAATTCTAATGGTGATGGTGATGGTGGCTGTTGTTCTCGGCTGTGAG -3' to produce the right fragment). The left fragment was digested with NotI and BamHI, and the right fragment with BamHI and EcoRI. The latter was then subcloned into the pcDNA3 vector (Invitrogen), after which the resulting plasmid was digested with BamHI and XbaI (whose recognition site is located at the 3'-region of the EcoRI site). The two fragments were then ligated into a NotI/XbaI-digested p3xFLAG-CMV-9 vector (Sigma-Aldrich) to generate construct p3xFLAG-CMV-9-LARGEdTM, which expresses a LARGE fusion protein (amino acids 34-756) tagged with a 3xFLAG at its N-terminus and Hisx6 at its C-terminus.

LARGEdTM DXD1

The construct harboring the DXD1 (D242N/D244N) mutations was generated by digesting p3xFLAG-CMV-9-LARGEdTM with EcoRI and XhoI, then treating it with T4 DNA polymerase (NEB) and allowing self-ligation. This strategy resulted in elimination of the EcoRV and NotI recognition sites derived from pcDNA3, in the construct p3xFLAG-CMV-9-LARGEdTM-delta. A DNA fragment harboring the DXD1 (D242N/D244N) mutations was amplified using 5'-phosphorylated primers (#3848: 5'-ATGGGCGTGGATAGCGGTTTGACTC-3' and #7604: 5'-ATTCGTGTTAAGGACGATGACTCTCTCCAG-3'), digesting the product with NotI, and then ligating it into NotI/EcoRV-digested p3xFLAG-CMV-9-LARGEdTM-delta vector to produce p3xFLAG-CMV-9-LARGEdTM-DXD1.

LARGEdTM DXD3

The construct harboring the DXD3 (D563N/D565N) mutations was generated using two-sided splicing involving overlapping extension. The left and right fragments were amplified using the primer pairs (#3000: 5'-AAGTTTCCTGGATCCCCAAT-3' and #7602: 5'-CATGGGCAGGAAGTTAATGTTAGACAGGAACAT-3' to generate the left fragment; and #7601: 5'-ATGTTCCTGTCTAACATTAACTTCCTGCCCATG-3' and #2999: 5'-CCTTTCGTCCAGACGTGGTA-3' to generate the right fragment). These PCR products were used as templates for a subsequent amplification using primers #3000 and #2999. The resulting band was digested with KpnI and cloned into KpnI-digested p3xFLAG-CMV-9-LARGEdTM vector to produce p3xFLAG-CMV-9-LARGEdTM-DXD3.

Generation of cell lines stably expressing LARGEdTM proteins
HEK293 cells were transfected with constructs p3xFLAG-CMV-9-LARGEdTM-WT, DXD1, and DXD3 (each of which contains a neomycin resistance cassette), using FuGENE 6 (Roche Applied Science), and selected in medium containing Geneticin (500 μg/ml, Invitrogen). Single colonies were isolated and analyzed for expression of the respective LARGEdTM protein, by immunoblotting with anti-FLAG M2 antibody (Sigma-Aldrich). The stable clones obtained in this way were adapted to serum-free medium 293SFMII (Invitrogen) and cultivated in CELLine bioreactors (CL1000, Argos Technologies).

Antibodies
Antibodies to α-DG glycan (IIH6) and core (goat20 or sheep5) epitopes have been described previously (4, 20). Anti-β-DG antibody 7D11 and anti-HS antibody 10E4 were purchased from Developmental Studies Hybridoma Bank at University of Iowa and from US Biological, respectively.

Glycoprotein enrichment, immunoblotting, and ligand overlays
Glycoprotein enrichment by wheat germ agglutinin (WGA)-agarose beads, immunoblotting, and ligand overlays were performed as described previously (20).

Compositional sugar analysis by GC-MS
Recombinant α-DG produced in HEK293 cells (21) was purified using agarose-bound Jacalin (Vector Laboratories) according to the manufacturer's instructions. The bound α-DG was eluted with 800 mM galactose and then desalted extensively. The purified α-DG was treated with PNGaseF, *O*-glycosidase, and α-2(3,6,8,9) neuraminidase, using the Enzymatic Protein Deglycosylation Kit (Sigma-Aldrich) according to manufacturer's protocol. Gas chromatography-mass spectrometry (GC-MS) analysis of trimethylsilyl derivatives was conducted by the Glycotechnology Core Resource (UCSD).

Xyloside treatment
Nearly confluent LARGE-expressing CHO cells were trypsinized and replated at a 1:5 dilution in fresh medium containing 1 mM Xyl-α-pNP (Calbiochem), and then cultured for 2 days.

Purification of LARGEdTM
LARGEdTM secreted into the culture medium by HEK293 cells was purified using the Talon metal affinity resin (Clontech) according to the manufacturer's instruction. The purity of the protein was confirmed by SDS-PAGE and Coomassie Brilliant Blue staining. The eluate was desalted for enzyme assay, using an Amicon Ultra-4 centrifugal filter unit (Millipore).

Analysis of LARGE enzymatic activity
The HPLC-based enzyme assay for LARGEdTM was performed using either Xyl-α-pNP or GlcA-β-MU (Sigma-Aldrich) as the acceptor. The sample was incubated for 1 or 2 h at 37ºC, with 5 mM UDP-GlcA or 0.5 mM UDP-Xyl and in 0.1 M 3-(N-morpholino)propanesulfonic acid (MOPS) buffer, pH 7.5, at 10 mM $MnCl_2$, 10 mM

$MgCl_2$, and 0.5% Triton X-100. The reaction was terminated by boiling for 5 min, and the supernatant was analyzed for (a) product, using a 4.6 x 250 mm GlycoSep N column (ProZyme), and (b) enzymatic activity, using a 4.6 x 250 mm Supelcosil LC-18 column (Supelco). For the GlycoSep N column, solvent A was acetonitrile, and solvent B was 250 mM ammonium formate, pH 4.4. For the LC-18 column, solvent A was 50 mM ammonium formate, pH 4.0, and solvent B was 80% acetonitrile in solvent A. The elution of pNP derivative and MU derivative was monitored by absorbance at 300 nm and by a fluorescence detector set at 325 nm for excitation and at 380 nm for emission, respectively. The enzymatic activity was examined in triplicate, and calculated as the peak area of the product.

In vitro LARGE enzymatic reaction using *LARGE*^{myd} mouse skeletal muscle

WGA-enriched glycoproteins from *LARGE*^{myd} mouse skeletal muscle were incubated overnight at 37ºC with LARGEdTM and 10 mM UDP-GlcA plus 10mM UDP-Xyl, in 0.1 M MOPS, pH 7.5, at 10 mM $MgCl_2$ and 0.5% Triton X-100. The reaction product was subjected to immunoblotting or ligand overlay.

Separation and purification of products of LARGE-catalyzed reaction

A large-scale reaction was carried out with 10 mM each of UDP-GlcA and UDP-Xyl, at 37ºC for 7 h, and the sample was separated by running it over two Superdex Peptide 10/300 gel-filtration columns (GE Healthcare) in tandem, using isocratic elution with 50 mM ammonium bicarbonate at a flow rate of 0.15 ml/min. The collected peak samples were lyophilized and dissolved in 50 mM ammonium formate, pH 4.0 and further purified over an LC-18 column.

LTQ XL liner ion trap MS and HPAEC-PAD analyses

The glycan samples were dissolved in 50% acetonitrile/water (v/v) and directly infused into an LTQ XL liner ion-trap mass spectrometer (Thermo Scientific, Inc.) at 5 µl/min, using a syringe pump. The samples were ionized using negative nanospray ionization. Capillary temperature and needle voltage were 200°C and -4.5-5 kV, respectively. Collisions for MS^n were carried out with an isolation window of 3.0 u and a normalized collision energy of 20-35%.

MALDI-TOF MS/MS

α-cyano-4-hydroxycinnamic acid (saturated in a mixture of acetonitrile and 0.1% TFA in 1:1 v/v) was used as the matrix. Mass spectra were obtained using a Bruker ultrafleXtreme MALDI-TOF/TOF mass spectrometer in negative linear mode. MALDI targets were prepared by spotting 1.0 µl of a mixture of the sample and the matrix (1:1 v/v ratio) onto an MTP anchorchip 800/384 plate (Bruker). Angiotensin I and a peptide of molecular weight 1500 kD, were used as external standards. MS/MS spectra were obtained in LIFT mode.

NMR study

After hydroxyl hydrogens of the sample fractionated by gel filtration and LC-18 chromatographies were replaced with deuterium (repeated dissolving of the sample in 99.9% D_2O followed by lyophilisation), the samples were dissolved in 10 mM $NaPO_4$

buffer, pH 6.5, in 100% D_2O and used for the NMR studies. ^{1}H homonuclear two-dimensional DQF-COSY, TOCSY (fig. S11), and ROESY experiments, and $^{1}H/^{13}C$ heteronuclear two-dimensional HMQC and HMBC experiments were carried out using a Bruker Avance II 800 MHz spectrometer equipped with a cryoprobe. NMR spectra were processed using the NMRPipe package, and analyzed using NMRView.

Flow cytometry

CHO, pgsI-208, pgsA-745 cells (22) or xyloside-treated cells were analyzed by flow cytometry using IIH6, CORE (goat20), or 10E4, as described previously (4).

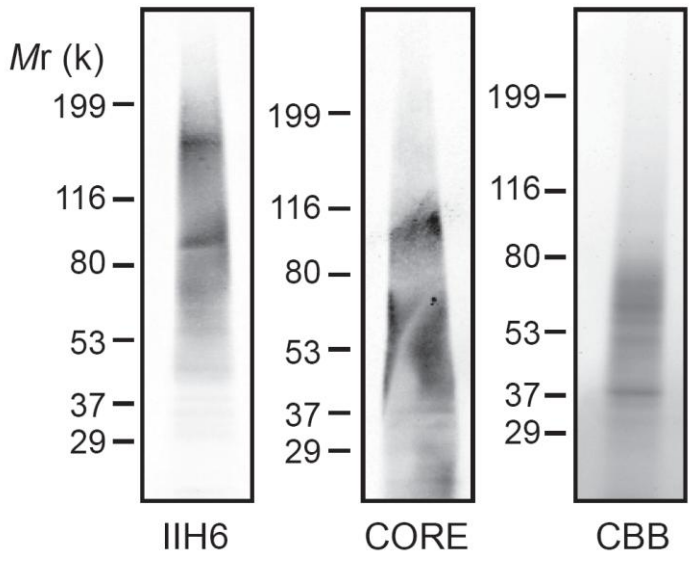

Fig. S1.

HEK293 cells stably expressing both α-DG and LARGE produce functionally modified recombinant α-DG. Recombinant α-DG secreted into the serum-free medium was purified using agarose-bound Jacalin. The eluate was subjected to immunoblotting with the IIH6 and CORE antibodies. CBB, Coomassie Brilliant Blue staining.

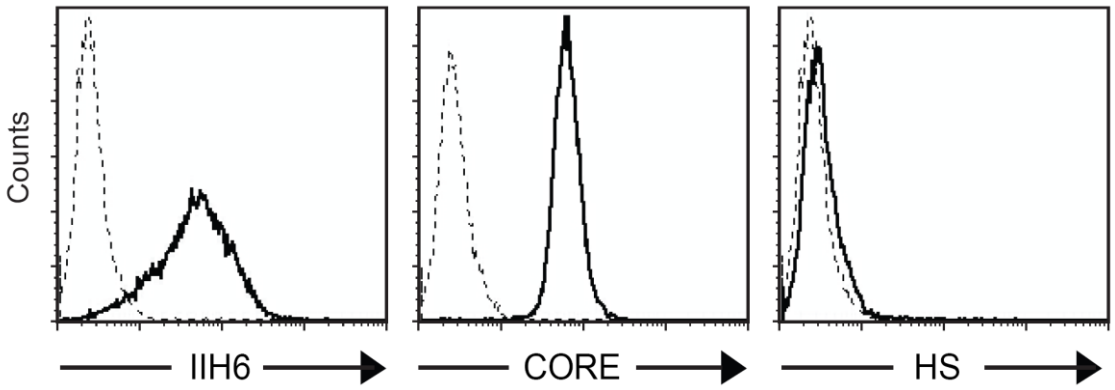

Fig. S2.

GAG-deficient CHO mutant pgsA-745 cells retain the ability to functionally modify α-DG. Cells were stained with the IIH6, CORE, or HS antibody, and then analyzed by flow cytometry. Dashed line, secondary antibody alone.

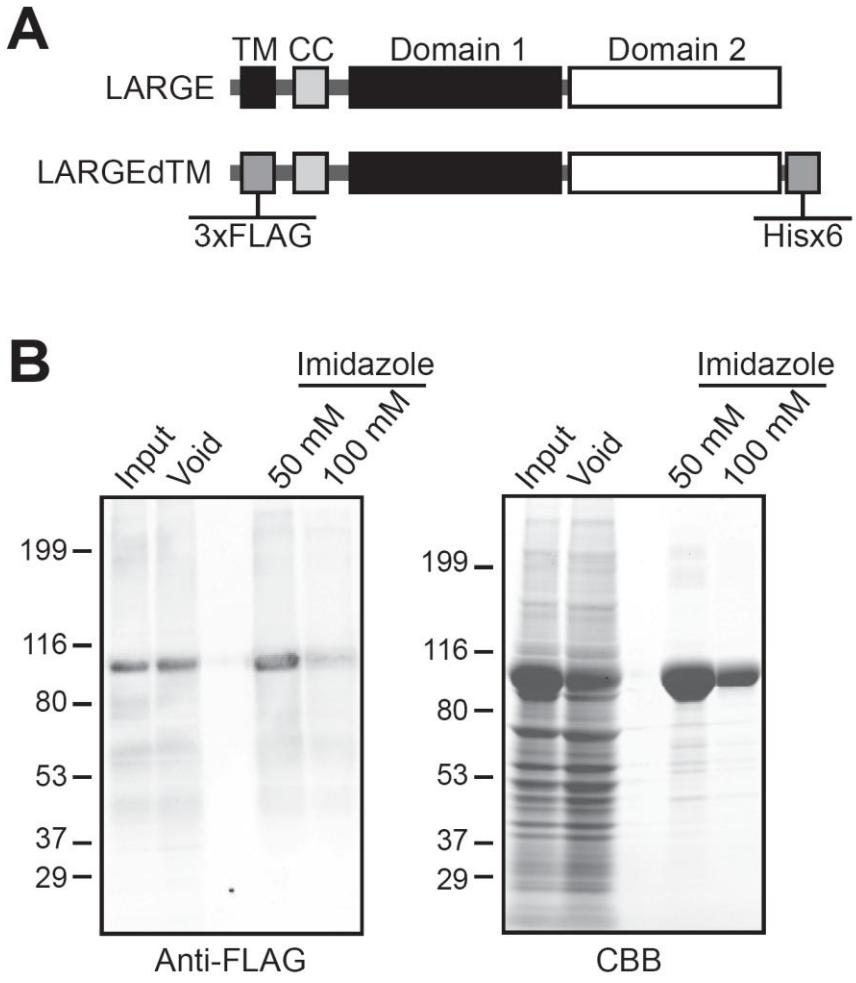

Fig. S3.

Purification of LARGEdTM. (A) Schematic representation of the LARGEdTM construct used in the LARGE enzymatic activity assay. The transmembrane (TM) sequence was replaced with a 3xFLAG tag sequence and the C-terminus was modified with a Hisx6 tag. CC, Coiled-coil domain. (B) The recombinant protein expressed in the culture medium was purified on a Talon metal affinity resin, and the eluates were analyzed by immunoblotting with anti-FLAG antibody. CBB, Coomassie Brilliant Blue staining.

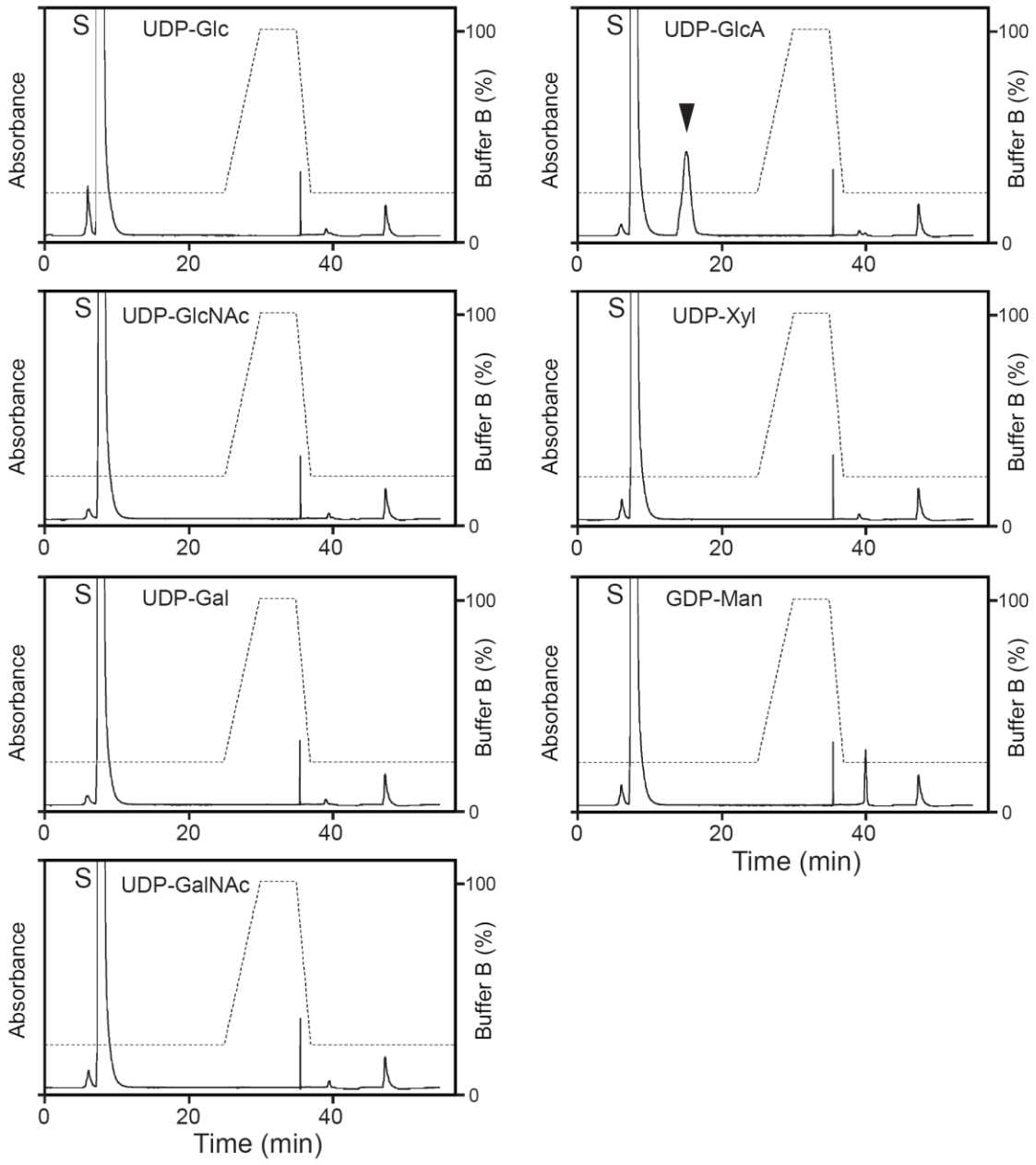

Fig. S4.

HPLC elution profile of the product of the LARGEdTM-catalyzed reaction when Xyl-α-pNP served as the acceptor. Xyl-α-pNP was incubated with LARGEdTM and the donor sugar indicated in panel, and the reaction product was analyzed by HPLC using a GlycoSep N column (solid line). S, unreacted substrate. Arrowhead indicates a unique peak observed only in the presence of UDP-GlcA. Dashed line, %B buffer.

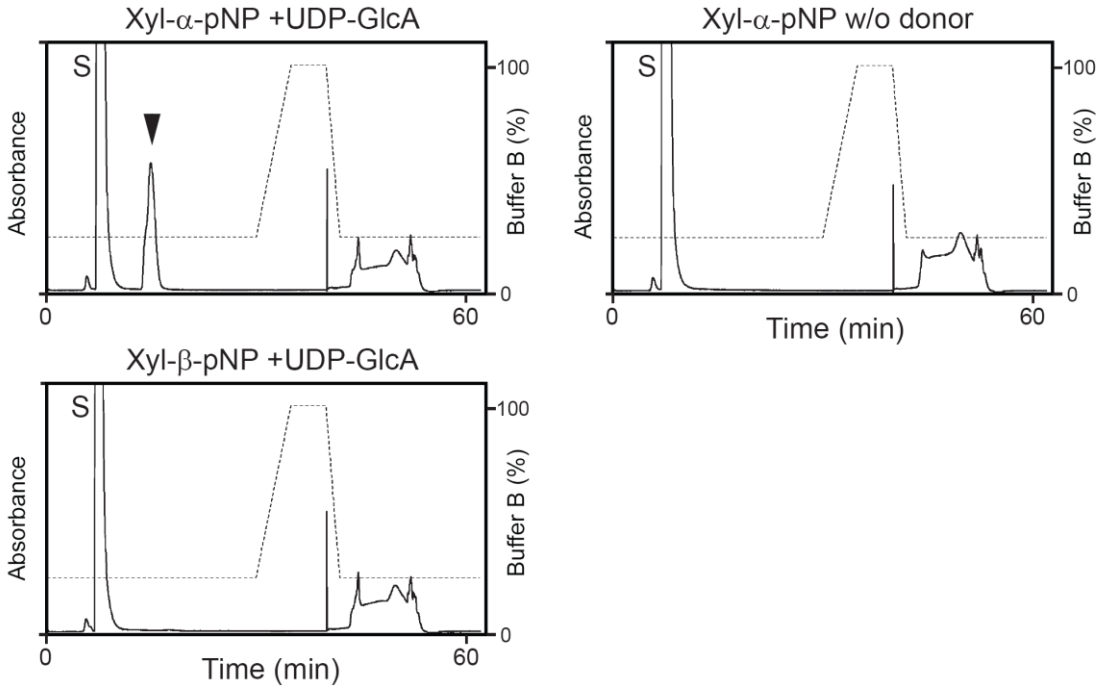

Fig. S5.

HPLC elution profile of the product of the LARGEdTM-catalyzed reaction when Xyl-α-pNP or Xyl-β-pNP served as the acceptor. Each Xyl-pNP form was incubated with LARGEdTM and UDP-GlcA, and the reaction product was analyzed by HPLC using a GlycoSep N column (solid line). S, unreacted substrate. Arrowhead indicates a unique peak observed only when Xyl-α-pNP serves as the acceptor, and UDP-GlcA is present. Dashed line, %B buffer.

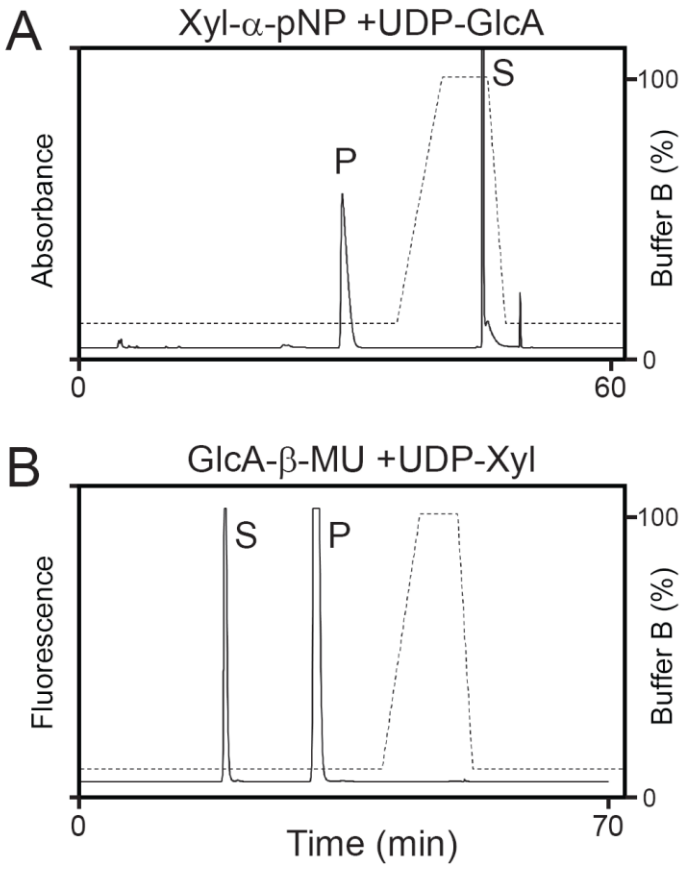

Fig. S6.

Isolation of the LARGEdTM-catalyzed reaction products for MS analysis. Product from Xyl-α-pNP (A) or GlcA-β-MU (B) was separated on an LC-18 column. Elution of the derivatives of pNP and MU was monitored by measuring absorbance at 300 nm (solid line in A) and fluorescence (solid line in B, detector set at 325 nm for excitation and 380 nm for emission), respectively. Dashed line, %B buffer. S, unreacted substrate. P, enzymatic product.

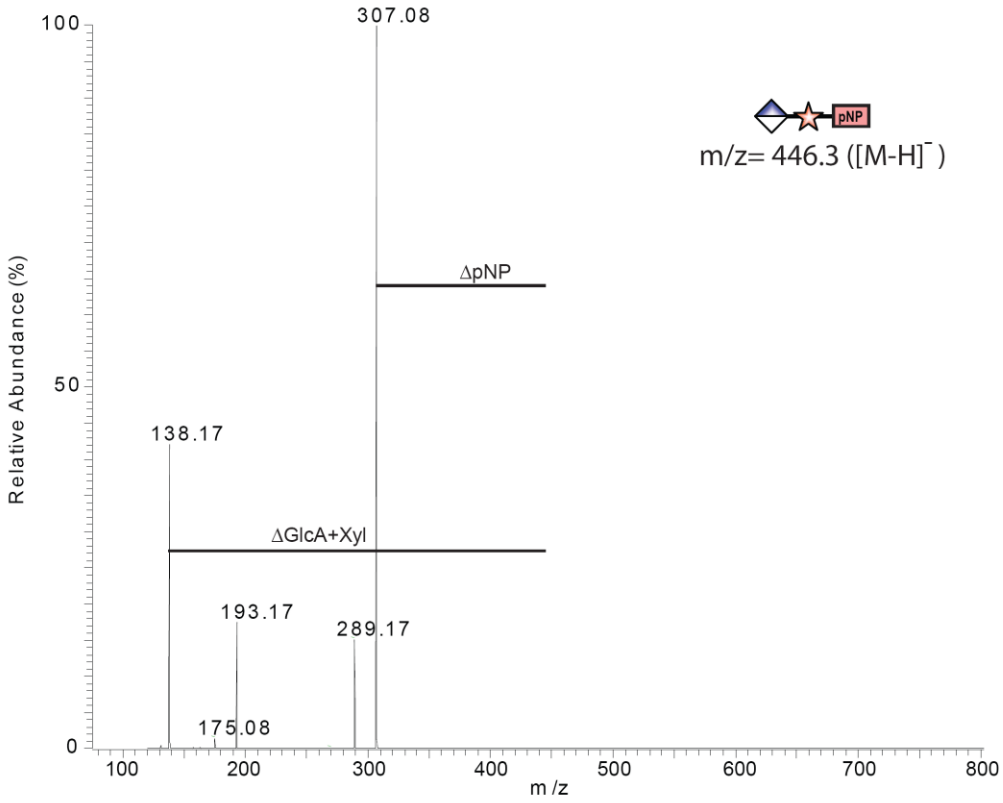

Fig. S7.

Nanospray ionization-linear ion-trap mass spectrometry in negative-ion mode. CID MS/MS spectrum derived from the parent ion [M-H]- (m/z 446.3). Star and diamond indicate Xyl and GlcA, respectively.

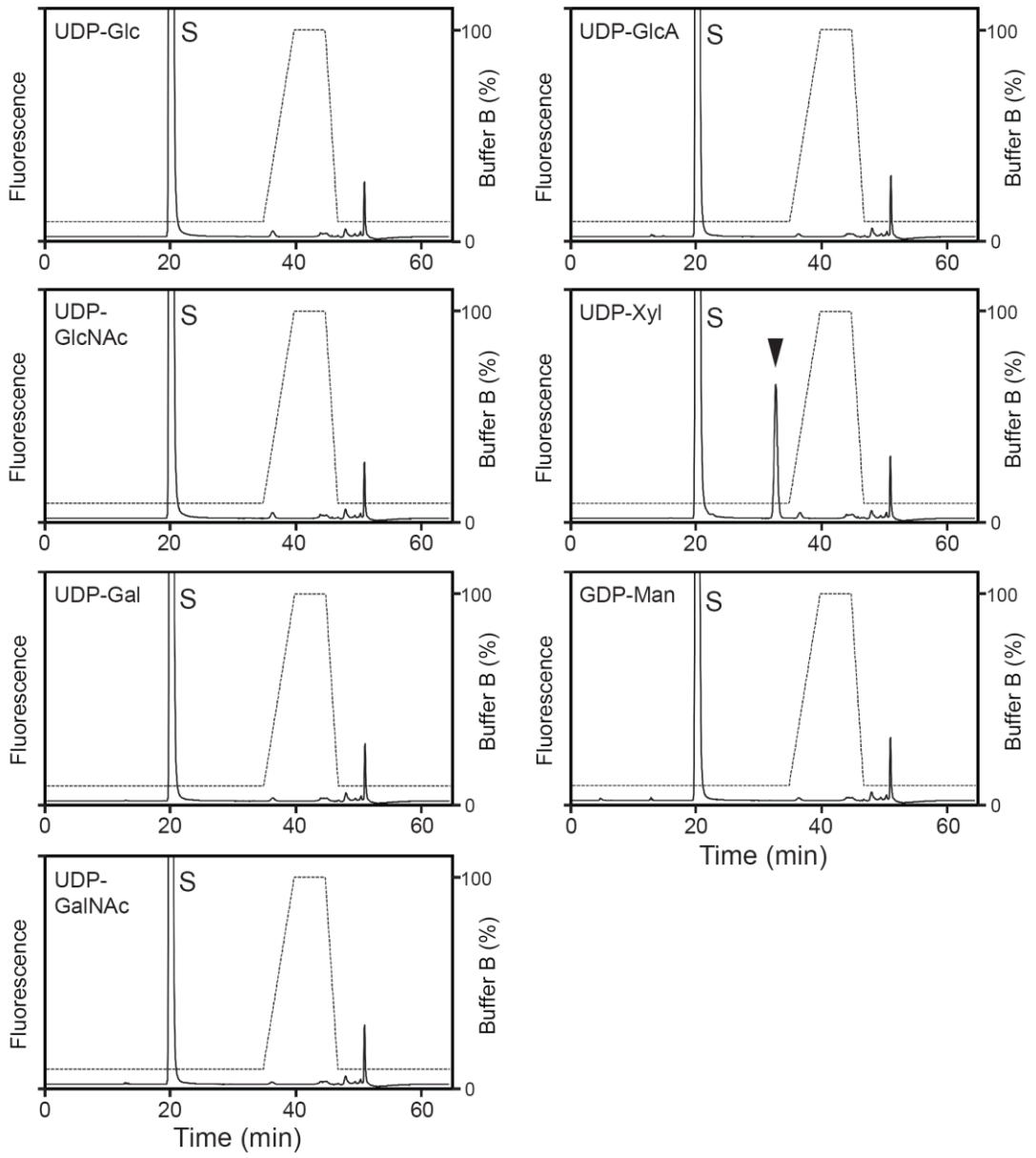

Fig. S8.

HPLC elution profile of the product of the LARGEdTM-catalyzed reaction when MU-β-GlcA served as the acceptor. MU-β-GlcA was incubated with LARGEdTM and the donor sugar indicated in panel, and the reaction product was analyzed by HPLC using an LC-18 column (solid line). S, unreacted substrate. Arrowhead indicates a unique peak observed only in the presence of UDP-Xyl. Dashed line, %B buffer.

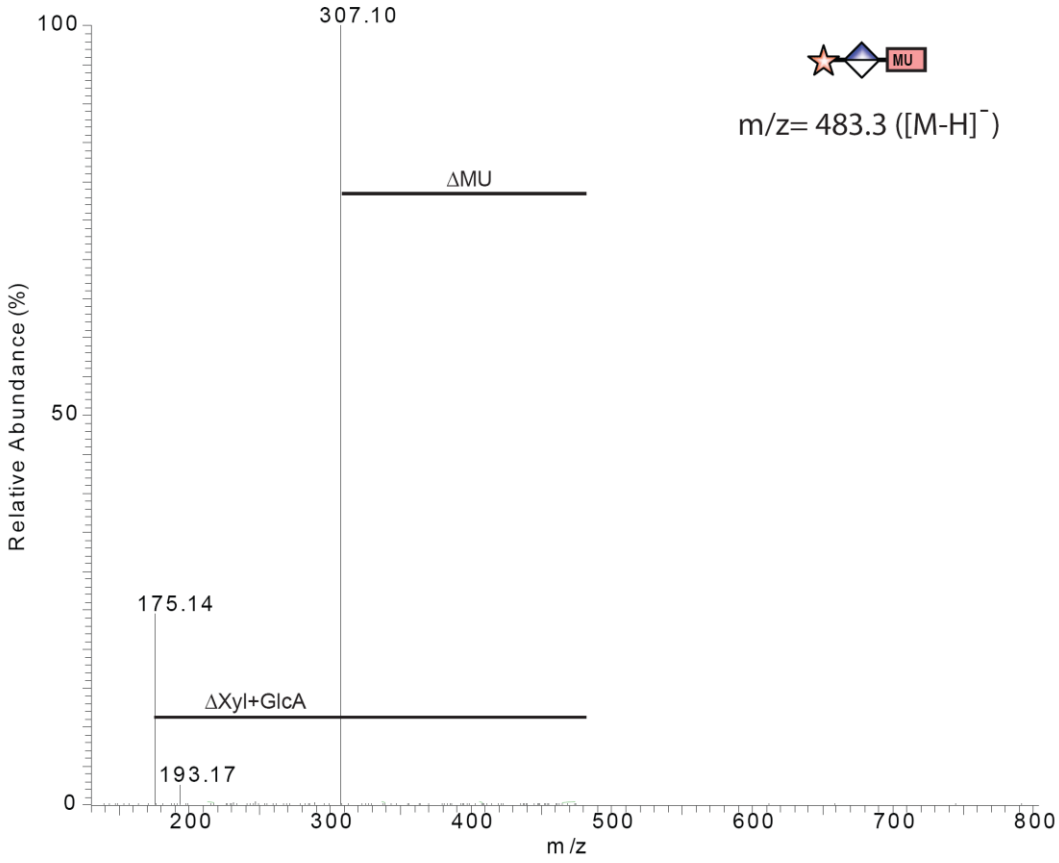

Fig. S9.

Nanospray ionization-linear ion trap mass spectrometry in negative ion mode. CID MS/MS spectrum derived from the parent ion [M-H]- (m/z 483.3). Star and diamond indicate Xyl and GlcA, respectively.

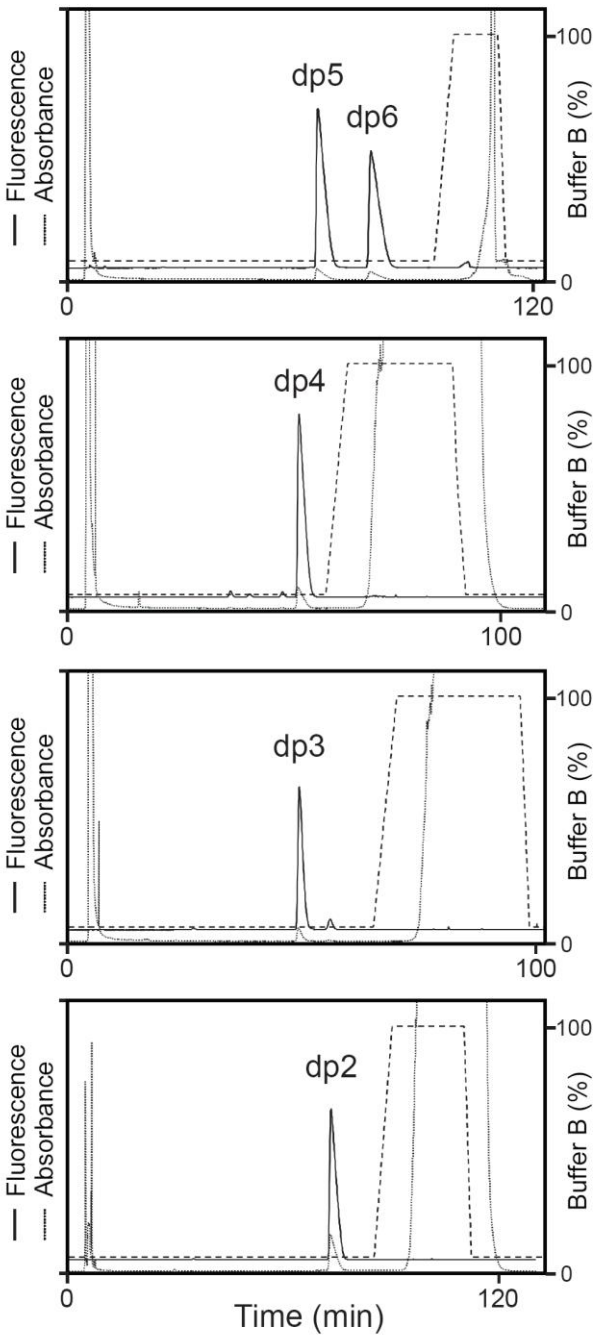

Fig. S10.

Purification of MU-β-GlcA derivatives by reversed-phase HPLC. Each peak isolated by gel-filtration (Fig. 4A) was further purified on an LC-18 column. Elution of the MU derivatives was monitored using a fluorescence detector set at 325 nm for excitation and 380 nm for emission (solid line). Dotted line, absorbance at 254 nm. Dashed line, %B buffer.

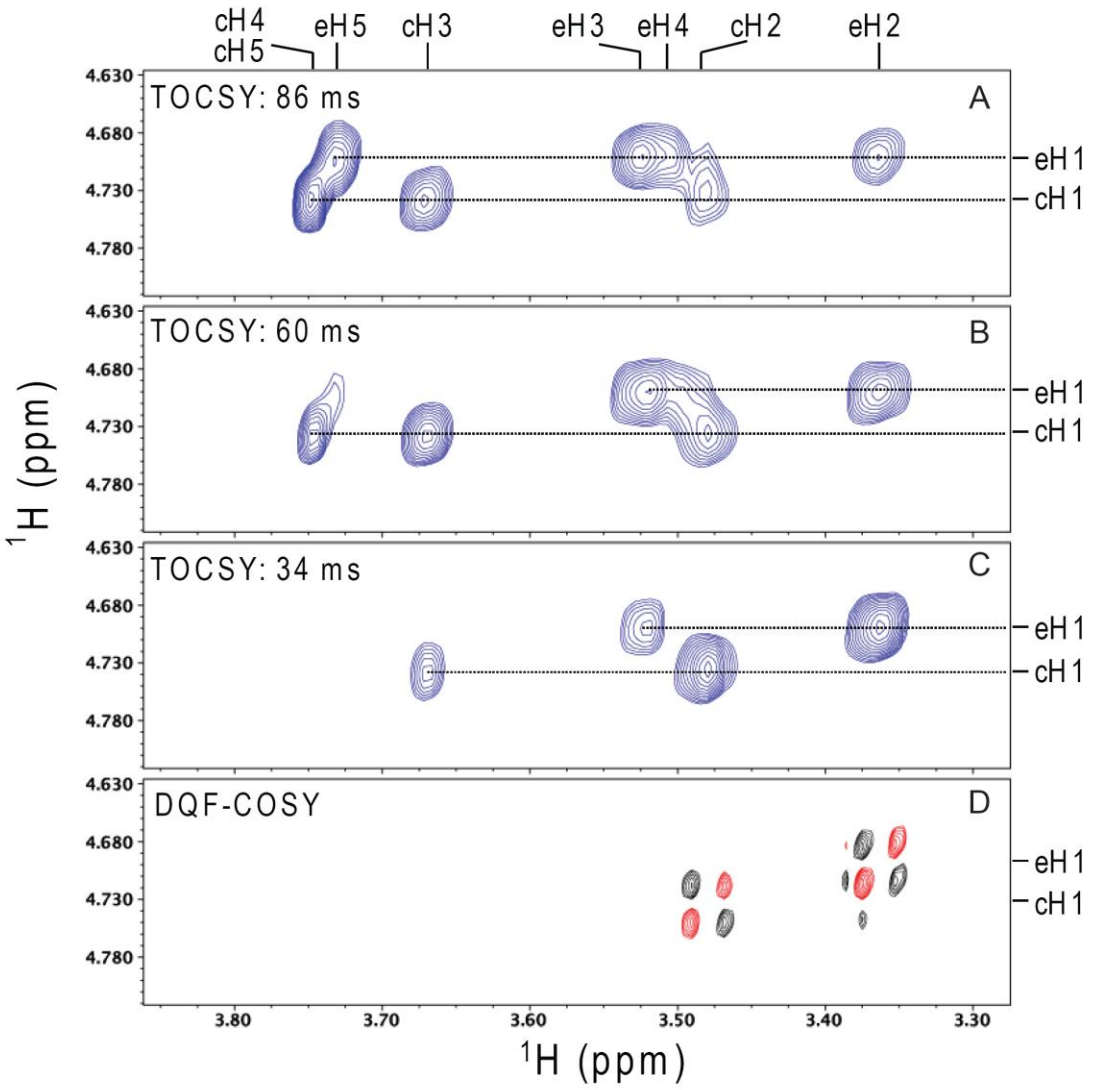

Fig. S11.

NMR analysis of dp5 at 15ºC. TOCSY (A-C) and DQF-COSY (D) spectra for the assignment of proton in subunit c and e. The assigned protons are indicated along the top and right sides of the panels. TOCSY mixing times of 34, 60, and 86 ms were used for spectra C, B, and A, respectively.

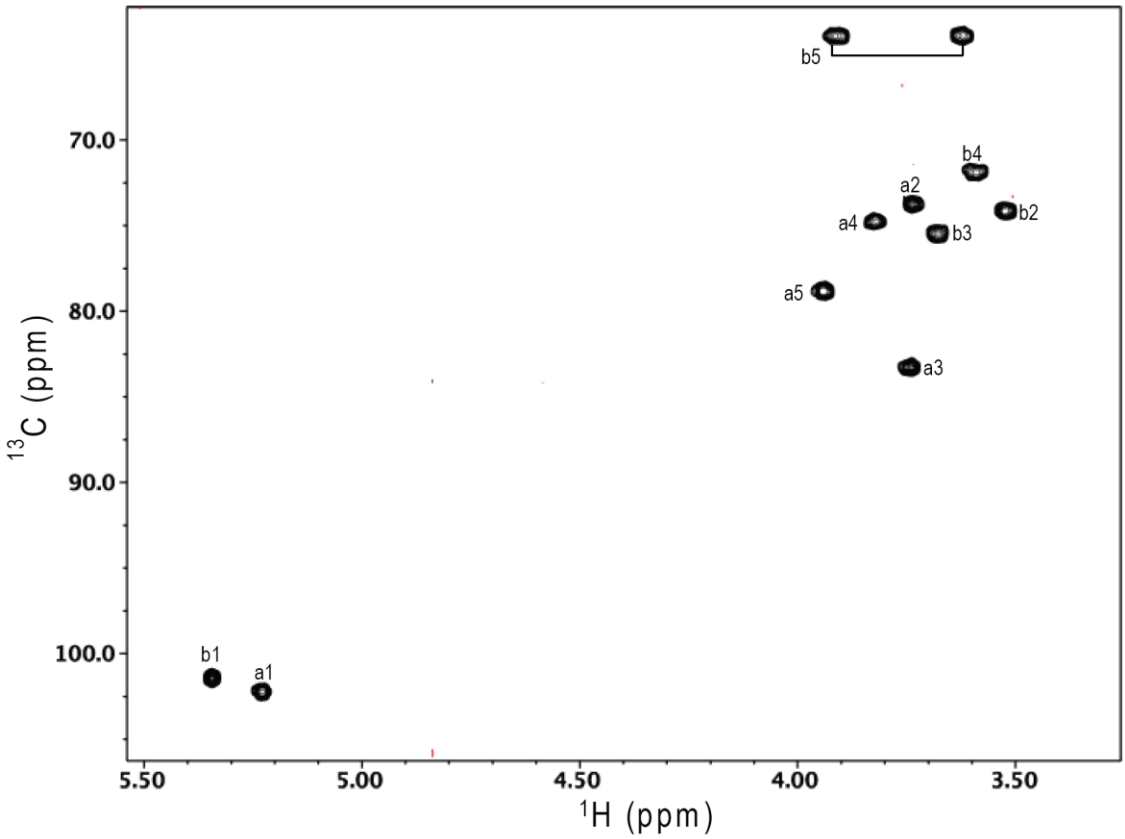

Fig. S12.

NMR analysis of product dp2 at 15ºC. HMQC spectrum, with the assigned cross peaks labeled with a letter indicating the subunit as designated in Fig. 4F, and a number indicating the position on that subunit.

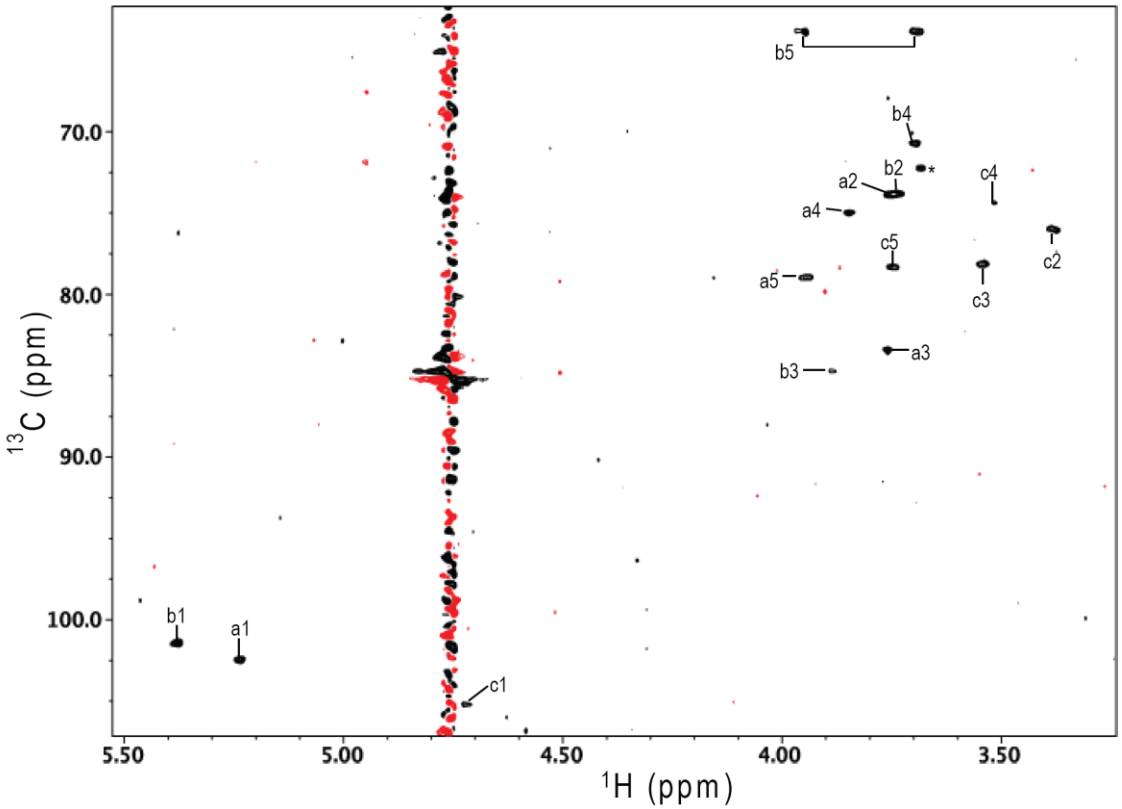

Fig. S13.

NMR analysis of product dp3 at 25ºC. Shown is the HMQC spectrum, with the assigned cross peaks labeled with a letter indicating the subunit as designated in Fig. 4F, and a number indicating the position on that subunit. The cross peak derived from sample impurities is indicated by an asterisk.

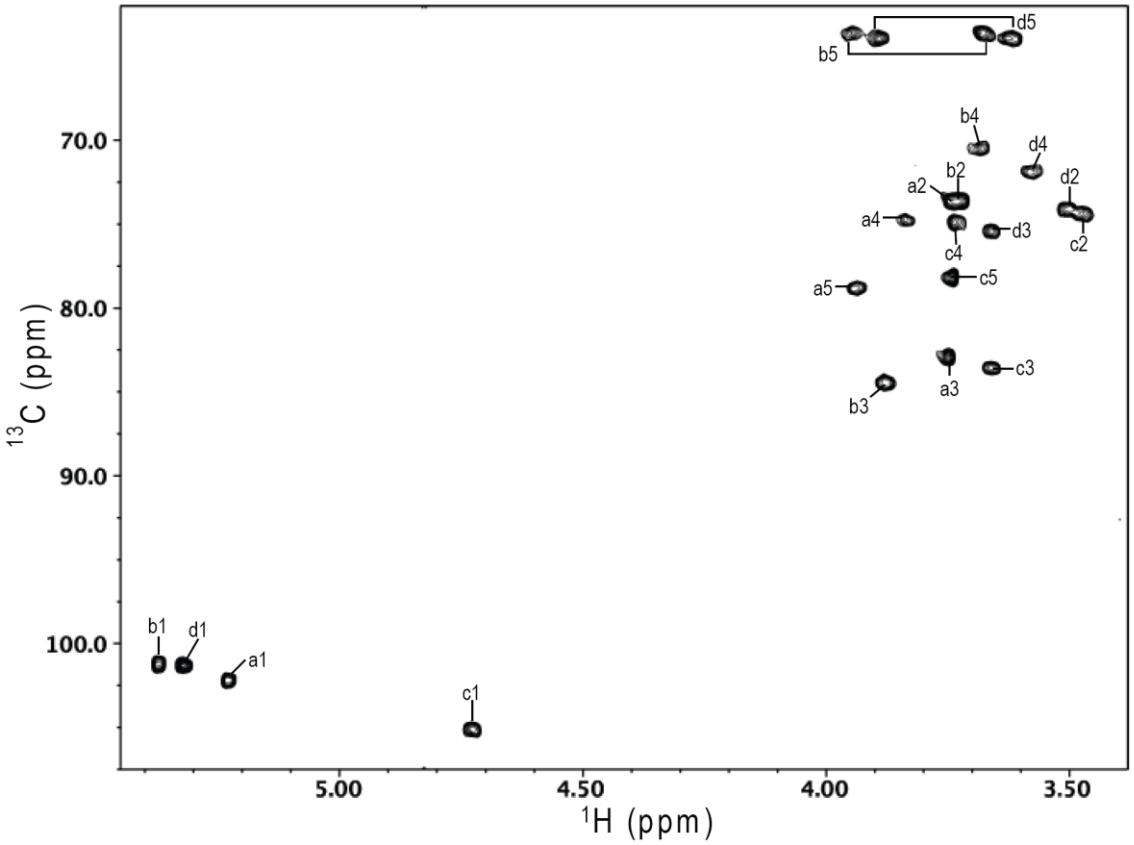

Fig. S14.

NMR analysis of product dp4 at 15ºC. Shown is the HMQC spectrum, with the assigned cross peaks labeled with a letter indicating the subunit designated in Fig. 4F, and a number indicating the position on that subunit.

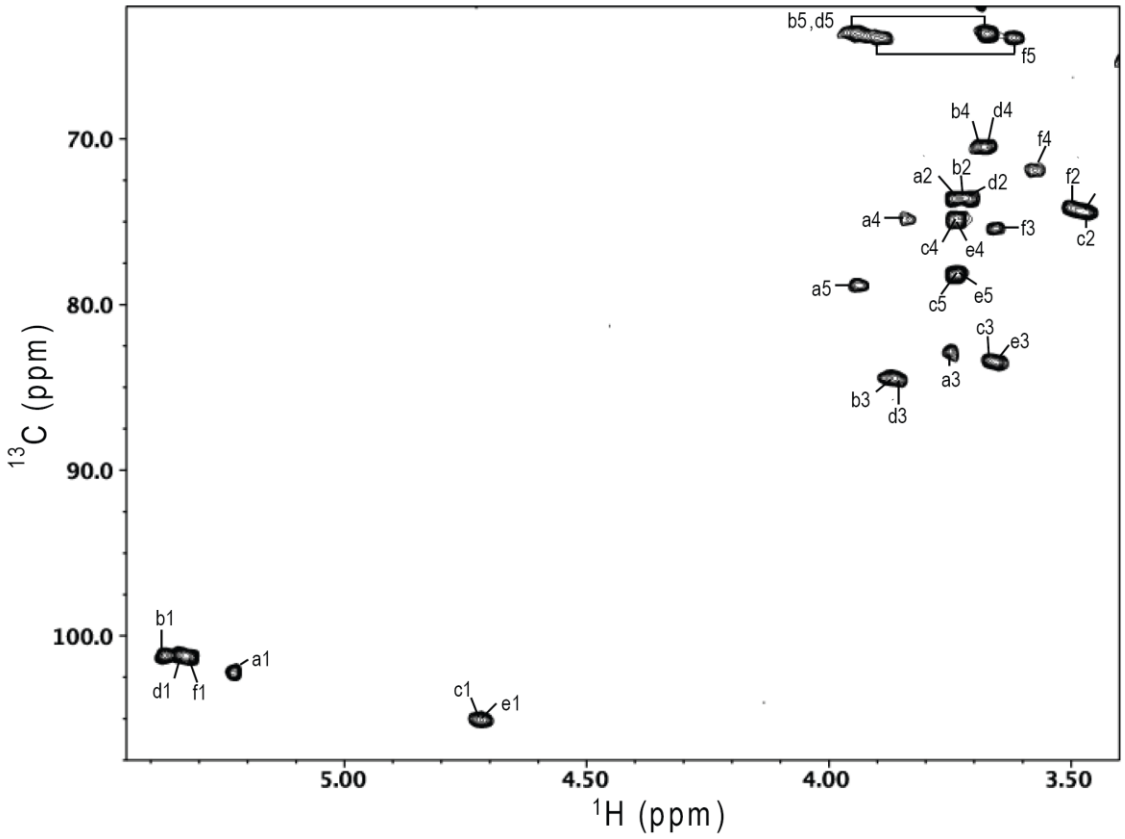

Fig. S15.

NMR analysis of product dp6 at 15ºC. Shown is the HMQC spectrum, with the assigned cross peaks labeled with a letter indicating the subunit designated in Fig. 4F, and a number indicating the position on that subunit.

Table S1. Chemical shifts (ppm) of the signals in the ^{1}H and ^{13}C NMR spectra of some of the enzymatic reaction products of the glycosyltransferase LARGE.

Products	$^{1}H/^{13}C$ (ppm)[a]										
	Sugar						Aromatic Ring[b]				
	1	2	3	4	5	6[b]	3	4-CH_3	6	7	9
dp2 (2 sugar units)											
→3)-β-D-GlcA-MU	5.24	3.76	3.76	3.84	3.95	-	6.28	2.47	7.76	7.13	7.13
a	102.6	74.1	83.9	75.0	78.9	177.7	113.9	20.7	129.3	116.3	106.4
α-D-Xyl-(1→	5.36	3.55	3.70	3.61	3.65, 3.91						
b	101.7	74.5	75.8	72.2	64.3						
dp3 (3 sugar units)											
→3)-β-D-GlcA-MU	5.23	3.76	3.76	3.85	3.95	-	6.30	2.47	7.78	7.16	7.15
a	102.4	73.9	83.4	75.0	79.0	177.7	114.1	20.7	129.5	116.7	106.8
→3)-α-D-Xyl-(1→	5.38	3.74	3.88	3.70	3.69, 3.95						
b	101.4	73.9	84.7	70.7	63.9						
β-D-GlcA-(1→	4.72	3.38	3.54	3.51	3.75						
c	105.2	76.0	78.1	74.4	78.3						
dp4 (4 sugar units)											
→3)-β-D-GlcA-MU	5.23	3.75	3.75	3.84	3.94	-	6.28	2.46	7.76	7.13	7.13
a	102.2	73.7	82.9	74.7	78.9	177.7	113.9	20.5	129.2	116.3	106.4
→3)-α-D-Xyl-(1→	5.37	3.73	3.88	3.68	3.68, 3.95						
b	101.2	73.7	84.5	70.5	63.6						
→3)-β-D-GlcA-(1→	4.72	3.48	3.66	3.74	3.74						
c	105.1	74.4	83.6	74.9	78.2						
α-D-Xyl-(1→	5.32	3.50	3.66	3.58	3.62, 3.89						
d	101.3	74.1	75.5	71.9	64.0						
dp5 (5 sugar units)											
→3)-β-D-GlcA-MU	5.23	3.75	3.75	3.84	3.94	-	6.28	2.46	7.76	7.13	7.13
a	102.2	73.6	83.0	74.7	78.8	177.7	113.9	20.5	129.2	116.3	106.3
→3)-α-D-Xyl-(1→	5.38	3.74	3.87	3.69	3.68, 3.95						
b	101.2	73.6	84.4	70.5	63.6						
→3)-β-D-GlcA-(1→	4.72	3.48	3.67	3.75	3.75						
c	105.0	74.4	83.4	74.9	78.2						
→3)-α-D-Xyl-(1→	5.35	3.72	3.86	3.68	3.67, 3.94						
d	101.1	73.6	84.5	70.6	63.6						
β-D-GlcA-(1→	4.69	3.36	3.52	3.49	3.73						
e	104.9	75.8	77.9	74.4	78.2						
dp6 (6 sugar units)											
→3)-β-D-GlcA-MU	5.23	3.75	3.75	3.84	3.94	-	6.28	2.46	7.76	7.13	7.13
a	102.2	73.6	82.9	74.8	78.9	177.7	113.9	20.5	129.2	116.3	106.4
→3)-α-D-Xyl-(1→	5.38	3.73	3.87	3.68	3.67, 3.94						
b	101.2	73.6	84.5	70.5	63.7						
→3)-β-D-GlcA-(1→	4.72	3.47	3.67	3.74	3.75						
c	105.1	74.5	83.5	74.8	78.2						
→3)-α-D-Xyl-(1→	5.34	3.72	3.86	3.67	3.67, 3.94						

d	101.1	73.6	84.5	70.5	63.7
→3)-β-D-GlcA-(1→	4.72	3.47	3.65	3.73	3.73
e	105.1	74.4	83.5	74.8	78.2
α-D-Xyl-(1→	5.31	3.49	3.66	3.57	3.62, 3.89
f	101.3	74.2	75.4	71.8	63.9

[a] Chemical shifts at 15 ^{o}C for all the products except for dp3 which is at 25 ^{o}C.
[b] Assigned based on the overlay of HMQC and HMBC spectra.

References

1. A. Varki *et al*., Eds., *Essentials of Glycobiology* (Cold Spring Harbor Press, Cold Spring Harbor New York, ed. 2, 2009).

2. O. Ibraghimov-Beskrovnaya *et al*., Primary structure of dystrophin-associated glycoproteins linking dystrophin to the extracellular matrix. *Nature* **355**, 696 (1992). doi:10.1038/355696a0 Medline

3. R. Barresi, K. P. Campbell, Dystroglycan: from biosynthesis to pathogenesis of human disease. *J. Cell Sci.* **119**, 199 (2006). doi:10.1242/jcs.02814 Medline

4. T. Yoshida-Moriguchi *et al*., *O*-Mannosyl phosphorylation of alpha-dystroglycan is required for laminin binding. *Science* **327**, 88 (2010). doi:10.1126/science.1180512 Medline

5. C. Longman *et al*., Mutations in the human LARGE gene cause MDC1D, a novel form of congenital muscular dystrophy with severe mental retardation and abnormal glycosylation of alpha-dystroglycan. *Hum. Mol. Genet.* **12**, 2853 (2003). doi:10.1093/hmg/ddg307 Medline

6. C. Godfrey, A. R. Foley, E. Clement, F. Muntoni, Dystroglycanopathies: coming into focus. *Curr. Opin. Genet. Dev.* **21**, 278 (2011). doi:10.1016/j.gde.2011.02.001 Medline

7. M. Kanagawa *et al*., Molecular recognition by LARGE is essential for expression of functional dystroglycan. *Cell* **117**, 953 (2004). doi:10.1016/j.cell.2004.06.003 Medline

8. R. Barresi *et al*., LARGE can functionally bypass alpha-dystroglycan glycosylation defects in distinct congenital muscular dystrophies. *Nat. Med.* **10**, 696 (2004). doi:10.1038/nm1059 Medline

9. J. M. Ervasti, K. P. Campbell, A role for the dystrophin-glycoprotein complex as a transmembrane linker between laminin and actin. *J. Cell Biol.* **122**, 809 (1993). doi:10.1083/jcb.122.4.809 Medline

10. H. Yamada *et al*., Characterization of dp6troglycan-laminin interaction in peripheral nerve. *J. Neurochem.* **66**, 1518 (1996). doi:10.1046/j.1471-4159.1996.66041518.x Medline

11. H. Bakker *et al*., Functional UDP-xylose transport across the endoplasmic reticulum/Golgi membrane in a Chinese hamster ovary cell mutant defective in UDP-xylose Synthase. *J. Biol. Chem.* **284**, 2576 (2009). doi:10.1074/jbc.M804394200 Medline

12. N. B. Schwartz, L. Galligani, P. L. Ho, A. Dorfman, Stimulation of synthesis of free chondroitin sulfate chains by beta-D-xylosides in cultured cells. *Proc. Natl. Acad. Sci. U.S.A.* **71**, 4047 (1974). doi:10.1073/pnas.71.10.4047 Medline

13. P. M. Coutinho, E. Deleury, G. J. Davies, B. Henrissat, An evolving hierarchical family classification for glycosyltransferases. *J. Mol. Biol.* **328**, 307 (2003). doi:10.1016/S0022-2836(03)00307-3 Medline

14. M. Brockington *et al*., Localization and functional analysis of the LARGE family of glycosyltransferases: significance for muscular dystrophy. *Hum. Mol. Genet.* **14**, 657 (2005). doi:10.1093/hmg/ddi062 Medline

15. E. Hohenester, D. Tisi, J. F. Talts, R. Timpl, The crystal structure of a laminin G-like module reveals the molecular basis of alpha-dystroglycan binding to laminins, perlecan, and agrin. *Mol. Cell* **4**, 783 (1999). doi:10.1016/S1097-2765(00)80388-3 Medline

16. A. C. Combs, J. M. Ervasti, Enhanced laminin binding by alpha-dystroglycan after enzymatic deglycosylation. *Biochem. J.* **390**, 303 (2005). doi:10.1042/BJ20050375 Medline

17. P. K. Grewal, P. J. Holzfeind, R. E. Bittner, J. E. Hewitt, Mutant glycosyltransferase and altered glycosylation of alpha-dystroglycan in the myodystrophy mouse. *Nat. Genet.* **28**, 151 (2001). doi:10.1038/88865 Medline

18. D. Harrison *et al*., Crystal structure and cell surface anchorage sites of laminin alpha1LG4-5. *J. Biol. Chem.* **282**, 11573 (2007). doi:10.1074/jbc.M610657200 Medline

19. J. M. Rojek, K. P. Campbell, M. B. Oldstone, S. Kunz, Old World arenavirus infection interferes with the expression of functional alpha-dystroglycan in the host cell. *Mol. Biol. Cell* **18**, 4493 (2007). doi:10.1091/mbc.E07-04-0374 Medline

20. D. E. Michele *et al*., Post-translational disruption of dystroglycan-ligand interactions in congenital muscular dystrophies. *Nature* **418**, 417 (2002). doi:10.1038/nature00837 Medline

21. R. Han *et al*., Basal lamina strengthens cell membrane integrity via the laminin G domain-binding motif of alpha-dystroglycan. *Proc. Natl. Acad. Sci. U.S.A.* **106**, 12573 (2009). doi:10.1073/pnas.0906545106 Medline

22. J. D. Esko, T. E. Stewart, W. H. Taylor, Animal cell mutants defective in glycosaminoglycan biosynthesis. *Proc. Natl. Acad. Sci. U.S.A.* **82**, 3197 (1985). doi:10.1073/pnas.82.10.3197 Medline